Int. J. Electrochem. Sci., 11 **(2016)** 3815 - 3823

International Journal of
ELECTROCHEMICAL
SCIENCE
www.electrochemsci.org

First Principle Study of $Na_3V_2(PO_4)_2F_3$ for Na Batteries Application and Experimental Investigation

Jiguo Geng[1,2,*], *Feng Li*[2], *Shengqian Ma*[2], *Jing Xiao*[2] *and Manling Sui*[1*]

[1] Institute of Microstructure and Properties of Advanced Materials, Beijing University of Technology, Beijing 100124 China
[2] School of Physics and Electronic Engineering, Taishan University, Taian, Shandong, 271021, China
[*]E-mail: jiguogengbut@gmail.com mlsui@bjut.edu.cn

Received: 22 February 2016 / *Accepted:* 29 March 2016 / *Published:* 1 April 2016

In this paper, we used first principle calculation and experimental investigation for exploring the application of $Na_3V_2(PO_4)_2F_3$. The influence of insertion and extraction of Na was investigated using XRD analysis. Results indicated the $Na_3V_2(PO_4)_2F_3$ owing a stable lattice structure with unit cell volume. The desodiated phase of the $Na_3V_2(PO_4)_2F_3$ could remain a stable state until 700 ^oC, which provide an excellent stability for battery electrode fabrication. The experimental study showed the $Na_3V_2(PO_4)_2F_3$ could serve as an excellent candidate for rechargeable Na battery fabrication.

Keywords: $Na_3V_2(PO_4)_2F_3$; First priciple; Na battery; Electrode; XRD

1. INTRODUCTION

Because of the high energy density and excellent rechargeable property, Li-ion battery attracted lots attention for potential energy storage [1-7]. On the other hand, Na-ion battery was considered as an alternative approach for energy storage due to its lower cost and safety compared with Li-ion battery [8-17]. Although Na battery has some advantages than that of Li-ion battery, only small research efforts were made for Na ion battery compared with Li ion battery. Several electrode materials were investigated for potential application of Na ion battery such as phosphates/fluorophosphates [18, 19], alluaudites [20-22], Prussian blue based materials [23, 24] and NASICON framework compounds [25, 26]. However, the major drawback of Na ion battery which limited its commercial application is due to the larger size of the Na^+ (about three times larger than Li ions). It back the Na^+ cannot efficient intercalate into graphite, which lower the battery performance. Therefore, the strategies used for Li ion battery cannot be applied for Na ion battery. On the other

doi: 10.20964/110483

hand, due to the success of Li ion battery in many filed, lack of efforts were put into the Na ion battery for solving this problem. Despite the fact the success of Li ion battery, the development of Na ion battery makes the opportunity of open a next generation of the energy storage device.

One important issue of development of Na ion battery is design a suitable electrode material. Among the above mentioned materials, $Na_3V_2(PO_4)_2F_3$ was attracted considerable attention due to its excellent electrochemical property and simple synthesis. For example, Liu and coworkers demonstrated a carbon coated $Na_3V_2(PO_4)_2F_3$ nanocomposite and successfully used for Na ion battery and showed a long-term cycle life [27]. Song and co-workers mechanistic investigation of $Na_3V_2(PO_4)_2F_3$ for Na ion battery and showed excellent C-rate and cycling performances [28]. Zhang and co-worker demonstrated the $Na_3V_2(PO_4)_2F_3$ for advanced Na ion battery and showed high energy storage density [29]. $Na_3V_2(PO_4)_2F_3$ can be prepared using several methods. For example, Nicolas and co-worker demonstrated a spray-drying method for $Na_3V_2(PO_4)_2F_3$ synthesis [30]. Aguilar and co-worker demonstrated a Pechini synthesis method for preparing $Na_3V_2(PO_4)_2F_3$ [31]. Although current studies showed the promising electrochemical performance of $Na_3V_2(PO_4)_2F_3$, the detail of electrochemical property and its relation with structure has not been fully studied. In this work, we use first principle calculation and experimental study to reveal the structure of the $Na_3V_2(PO_4)_2F_3$ as well as its potential application for Na ion battery.

2. EXPERIMENTS

2.1 $Na_3V_2(PO_4)_2F_3$ synthesis

The preparation of $Na_3V_2(PO_4)_2F_3$ was using method developed by Barker et al. [32] with some modifications. The entire synthesis method includes two steps. VPO_4 was firstly synthesized using carbon black, V_2O_5 and $NH_4H_2PO_4$ as starting materials. 10 g VPO_4, 10 g $NH_4H_2PO_4$ and 1.5 g carbon black was mixed using a ball milling machine. Result mixture was calcinated at 700 ^oC for 3 h under argon condition. A dark black color powder was collected after ground the mixture solid. For second step, 4 g above black powder was mixed with 1.2 g NaF using a ball milling machine for 3 h. The mixture was then heated in 700 ^oC for 3 h under argon condition. After cool down, $Na_3V_2(PO_4)_2F_3$ was collected. The carbon content in the $Na_3V_2(PO_4)_2F_3$ is about 4%.

2.2 Characterization

The crystal information of prepared $Na_3V_2(PO_4)_2F_3$ was investigated using a X-ray powder diffraction (D-8 Advances) using Cu Kα radiation (λ = 1.5406 Å). The scan rate was set as 1°/min. The morphology of the $Na_3V_2(PO_4)_2F_3$ was observed using a SEM (FEI Quanta 200). The elemental information of the $Na_3V_2(PO_4)_2F_3$ was studied using a plasma atomic emission spectroscopy (ICP, Thermo Jarrel Ash). The thermogravimetric characterization (TGA) was tested using a DTG-50H (SHIMAZU) thermoanalzer.

2.3 Electrode fabrication and electrochemical property investigation

The Na ion battery electrode fabrication process was according the following procedure: the electrode was prepared using $Na_3V_2(PO_4)_2F_3$, acetylene black, and poly(vinylidene fluoride) in a NMP solvent. The electrode was fabricated on an Al foil followed by a dry process. A R2000 coin cell was then fabricated under argon condition using odium foil as an anode and a Celgard 2500 membrane as a separator. The electrochemical behaviour of the prepared battery was studied in the range of 2.0-4.5 V at various C-rates. The current rate of C/10 (12.82 mA/g) was used for investigating the charge/discharge property. In order to investigate the rate capability, the battery was firstly charged to 4.5 V and discharged to 2.0 V using different C rates.

2.4 Computation

Spin-polarized generalized gradient approximation (GGA) with Perdew–Burke–Ernzerhof (PBE) exchange-correlation parameterization to Density Functional Theory (DFT) was used for $Na_3V_2(PO_4)_2F_3$ calculation. The GGA + U approach was employed using U=5 eV and J=1 eV. A plane-wave basis with a kinetic energy cutoff of 300 eV was used.

3. RESULTS AND DISCUSSION

3.1 Characterization of $Na_3V_2(PO_4)_2F_3$

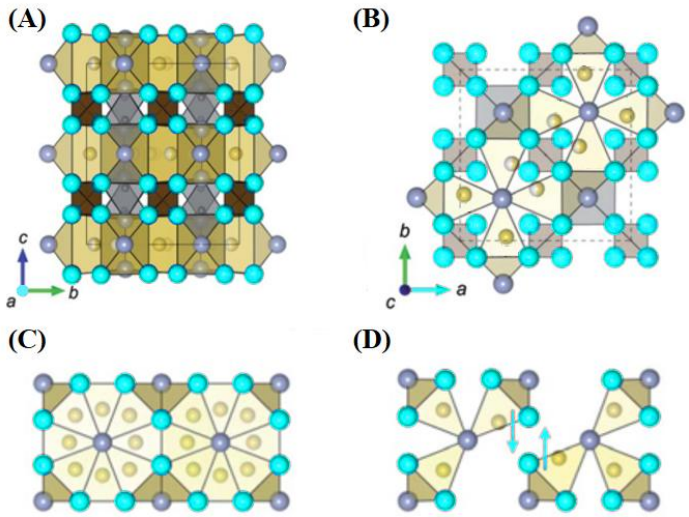

Figure 1. $Na_3V_2(PO_4)_2F_3$ structure in (A) *a* axis and (B) *c* axis direction. (C) All possible of Na sites. (D) Most stable Na ions configuration in $Na_3V_2(PO_4)_2F_3$.

The crystal structure of $Na_3V_2(PO_4)_2F_3$ at bc and ab plan were displayed in Figure 1 A and B, respectively. Bi-octahedral $V_2O_8F_3$ and tetrahedral PO_4 are constructed in $Na_3V_2(PO_4)_2F_3$ crystal framework. One F atom is bonded on the bi-octahedra where O atoms are bonded on the tetrahedral

PO_4, which provide channels in *a* and *b* directions for the intercalation of Na ions [26, 33-35]. The Na ions can occupy at two sites including surrounded by two F ions and four O ions or attached to the F apex-square pyramid. As shown in Figure 1 C, these sites formed repeated circle-like geometry in *ab* plane. Due to the larger space of the augmented triangular site, the calculated site energy by adding Na into each site was 55 meV, which is lower than that of the $NaV_2(PO_4)_2F_3$.

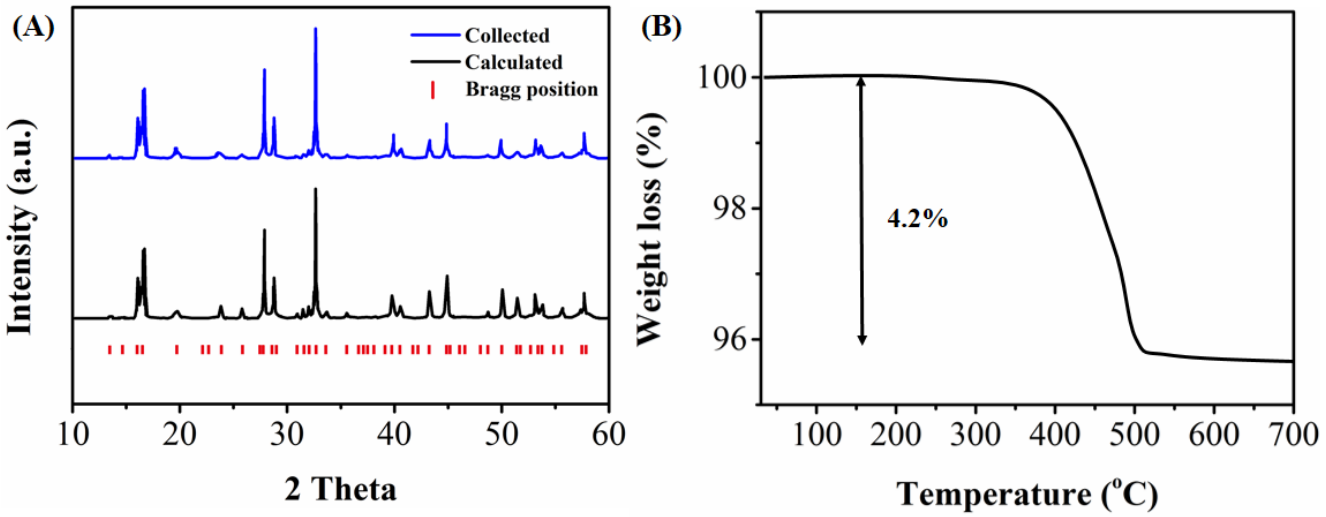

Figure 2. (A) XRD collected and calculated patterns of $Na_3V_2(PO_4)_2F_3$. (B) TGA curve of $Na_3V_2(PO_4)_2F_3$.

The structural relaxation of the Na configuration was studied as well. Figure 1D shows the most stable configuration of Na which consisted by three augmented triangular prismatic sites with eight Na sites. The Na ions showed a shift towards vacant Na sites due to the short distance between these Na sites. Figure 2A shows the XRD pattern of the $NaV_2(PO_4)_2F_3$. It can be seen that the $NaV_2(PO_4)_2F_3$ showed no impurities phase, indicating the residue carbon is in an amorphous state [36, 37].

Table 1. Lattice parameters of $NaV_2(PO_4)_2F_3$ and $Na_3V_2(PO_4)_2F_3$ using XRD characterization and DFT calculation.

Sample	Method	*a*	*c*	Volume (Å^3)
$NaV_2(PO_4)_2F_3$	XRD	8.905	10.698	860.22
	DFT	8.904	10.776	849.57
$Na_3V_2(PO_4)_2F_3$	XRD	9.035	10.701	977.19
	DFT	9.032	10.688	975.24

The refined lattice parameters were displayed in Table 1 and had a good agreement with previous studies [38-40] and the DFT results. Figure 2B shows the TGA cure of the $Na_3V_2(PO_4)_2F_3$, the carbon content in the $Na_3V_2(PO_4)_2F_3$ was determined as about 4.2 %. Moreover, the $Na_3V_2(PO_4)_2F_3$ showed an excellent stable thermal stability until 700 ^oC, indicating it's a safe electrode material for Na ion battery design.

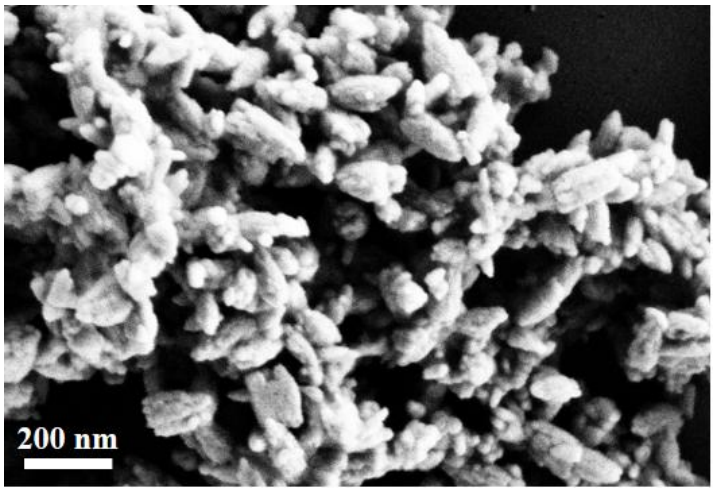

Figure 3. SEM image of as-prepared $Na_3V_2(PO_4)_2F_3$.

The morphology of the prepared $Na_3V_2(PO_4)_2F_3$ was characterized by SEM. As shown in Figure 3, the $Na_3V_2(PO_4)_2F_3$ displays a nanorod structure with slight aggregation. It can be observed that the $Na_3V_2(PO_4)_2F_3$ had a porous structure with some pores between the nanoparticles which is beneficial for the ions transportation.

3.2 Electrochemical behavior of $Na_3V_2(PO_4)_2F_3$

Figure 4A displays the rechargeable profiles of $Na_3V_2(PO_4)_2F_3$ cathode constructed Na battery. It can be seen that the charge/discharge curves of the $Na_3V_2(PO_4)_2F_3$ show two plateaus at voltages of 3.4 and 4.1 V. In comparison, the redox couple of V^{3+}/V^{4+} in $Na_xV_2(PO_4)_2F_3$ is about 3.95 V. The redox voltages of V_2O_5, LiV_3O_8, Li_2-$xNaV_2(PO_4)_3$ and $Li_{1-x}Na_2FeV(PO_4)$ are 2.7, 3.5, 3.8 and 3.7, respectively [41-43]. This behavior of the $Na_3V_2(PO_4)_2F_3$ can be ascribed to the superior inductive effects of anion groups such as the F ion and P ion, which shift the equilibrium potential [44]. This behavior suggests the $Na_3V_2(PO_4)_2F_3$ had a higher energy density, which makes the Na ions battery could have better performance than that of the Li ion battery. Figure 4B shows the cycle performance of the $Na_3V_2(PO_4)_2F_3$, the results indicated that the capacity could remain a very high level after 50 charge/discharge cycles. This performance was comparable with many recent reported Li ion batteries [15, 45-49]. It can be seen that the development of the Na ions battery is essential for alternative energy supply strategy design. The possible reason for the high rechargeable performance can be ascribed to the unique crystal structure change of the $Na_3V_2(PO_4)_2F_3$ during the ions movement. In

order to confirming the crystal change during the electrochemical reaction process, we used first-principles calculation for analyzing the electrochemical property of the $Na_xV_2(PO_4)_2F_3$. x=1, 2. 3 was calculated in this study. The average voltage was calculated as 3.91 V, which had a good agreement with the experimental result. We also removed the Na ions during the calculation in order to determine the valence band of the material at x values equal to 1, 2 and 3.

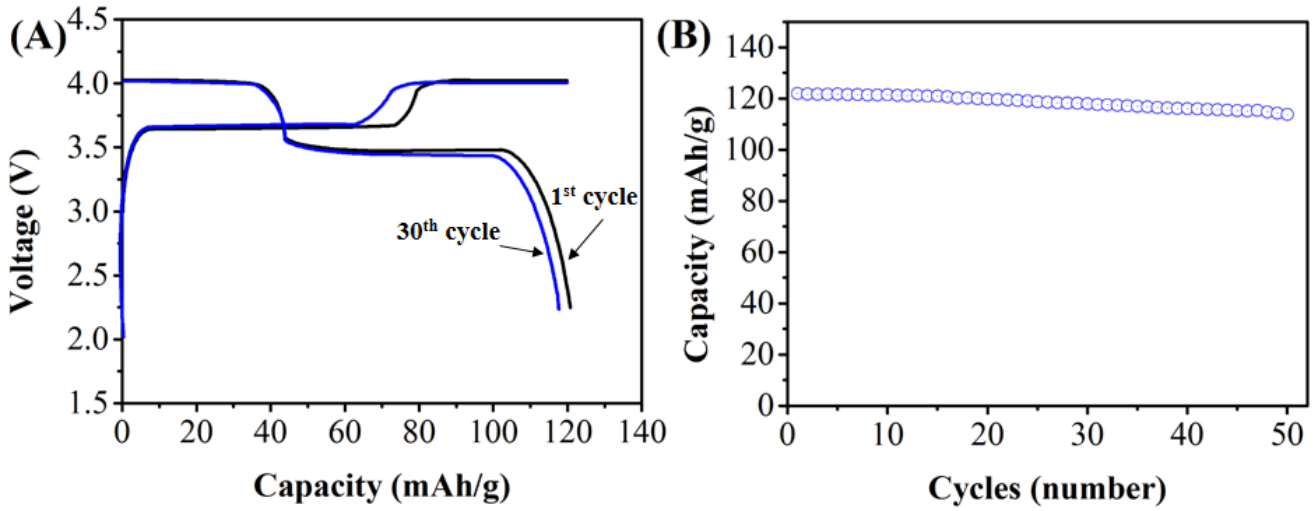

Figure 4. (A) Charge/discharge curves of the $Na_3V_2(PO_4)_2F$. (B) 50 charge/discharge cycle performance of the $Na_3V_2(PO_4)_2F_3$.

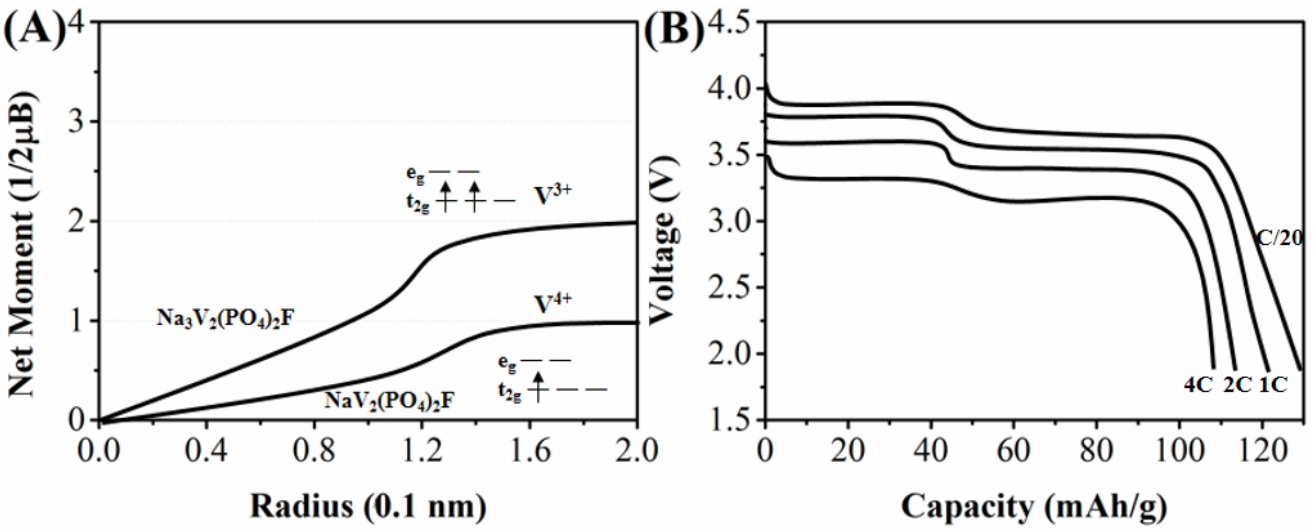

Figure 5. (A) Integrated spin as a function of integration radius around vanadium ions for $NaV_2(PO_4)_2F_3$ and $Na_3V_2(PO_4)_2F_3$. (B) Rate capability performance of $Na_3V_2(PO_4)_2F_3$.

The oxidation status of the V can be confirmed by integrating the electron spin around the V atom [50]. Figure 5A shows the integrated spin as a function of integration radius around V ions in $Na_xV_2(PO_4)_2F_3$ when x value equal to 1 and 3. As shown in the figure, the net spin moments were

converged into 1 and 2 for $NaV_2(PO_4)_2F_3$ and $Na_3V_2(PO_4)_2F_3$ at 1.6 Å, respectively. Therefore, electrochemical redox reaction of the $NaV_2(PO_4)_2F_3$ and $Na_3V_2(PO_4)_2F_3$ are ascribed to the redox of the V^{3+}/V^{4+}, which is the 3d band of the V ions.

As the two plateaus of the $Na_xV_2(PO_4)_2F_3$ is about 0.5 V, the Na ions may participate in two different environments. As mentioned in the Figure 1, three Na ions site are available in the crystallographica, however, the Na ion at Na2 site is not stable as the Na ion in the Na1 site due to the Na ion at Na2 site is shifted from the stable position, which make the Na ion at Na2 site has a higher chemical potential than that of the Na ion in Na1 site. Therefore, the Na ion at different sites will participates in the different stages of the charge and discharge process. Thus, we have reason to believe that after one Na ion participate in the redox reaction, other two Na ions could reorganized there position to form a more stable configuration. The distance of the Na ions will increase due to the unstable short Na–Na distance, which makes the second plateaus during the charge/discharge curve. We used first-principles calculation to verify this hypothesis. In terms of the $Na_2V_2(PO_4)_2F_3$, reorganization of Na ions in the Na sites was allowed and the chemical potential for the most stable configuration is about ―5.698eV, which is slightly lower than that of the $Na_2V_2(PO_4)_2F_3$ (―5.514 eV). This calculation also had a good agreement with the result collected in the experiment.

The rate capability of the $Na_3V_2(PO_4)_2F_3$ was also investigated and the results were shown in Figure 5B. It can be seen that the $Na_3V_2(PO_4)_2F_3$ performed more than 125 mAh/g at the C/20 rate and remained more than 80% capacity at 4C rate. This performance can be ascribed to the porous structure of the $Na_3V_2(PO_4)_2F_3$, low volume change and distortion of the crystal lattice upon charging/discharging which facilitates the fast diffusion of Na ions.

4. CONCLUSIONS

To sum up, we demonstrated a $Na_3V_2(PO_4)_2F_3$ cathode material in a Na ion battery through computation and experimental methods. The structural and electrochemical properties of the $Na_3V_2(PO_4)_2F_3$ were investigated. Results revealed that the $Na_3V_2(PO_4)_2F_3$ owing an outstanding charge/discharge, cyclability, rate capability and high redox potential, which make it most suitable for design Na ion battery electrode material.

ACKNOWLEDGMENTS
This work was supported by the National Natural Science Foundation of China (No.61204051). The numerical calculations in this paper have been done on the computing system in the Computing Center of School of Physics and Electronic Engineering of Taishan University of China.

References

1. C. Liang, D. Fang, Y. Cao, G. Li, Z. Luo, Q. Zhou, C. Xiong and W. Xu, *Journal of colloid and interface science*, 439 (2015) 69
2. B.D. Levin and D.A. Muller, *Microscopy and Microanalysis*, 21 (2015) 1549

3. W. Xu, G. Zhang and B. Li, *Applied Physics Letters*, 106 (2015) 173901
4. M. Bergman, A. Bergfelt, B. Sun, T. Bowden, D. Brandell and P. Johansson, *Electrochimica Acta*, 175 (2015) 96
5. Y. Chen, S. Sun, X. Wang and Q. Shi, *J Phys Chem C*, 119 (2015) 25719
6. Q. Zhu, H. Hu, G. Li, C. Zhu and Y. Yu, *Electrochimica Acta*, 156 (2015) 252
7. J. Li, C. Daniel, S.J. An and D. Wood, *MRS Advances*, (2015) 1
8. D. Kundu, R. Tripathi, G. Popov, W. Makahnouk and L.F. Nazar, *Chemistry of Materials*, 27 (2015) 885
9. Y. Zhang, P. Zhu, L. Huang, J. Xie, S. Zhang, G. Cao and X. Zhao, *Adv Funct Mater*, 25 (2015) 481
10. H. Usui, S. Yoshioka, K. Wasada, M. Shimizu and H. Sakaguchi, *ACS applied materials & interfaces*, 7 (2015) 6567
11. S. Renault, V.A. Mihali, K. Edström and D. Brandell, *Electrochemistry communications*, 45 (2014) 52
12. L. Xiao, Y. Cao, J. Xiao, W. Wang, L. Kovarik, Z. Nie and J. Liu, *Chemical Communications*, 48 (2012) 3321
13. Z. Shadike, M.-H. Cao, F. Ding, L. Sang and Z.-W. Fu, *Chemical Communications*, 51 (2015) 10486
14. Y. Bai, Z. Wang, C. Wu, R. Xu, F. Wu, Y. Liu, H. Li, Y. Li, J. Lu and K. Amine, *ACS applied materials & interfaces*, 7 (2015) 5598
15. K. Li, F. Shua, J. Zhang, K. Chen, D. Xue, X. Guo and S. Komarneni, *Ceram. Int.*, 41 (2015) 6729
16. J.K. Barillas, J. Li, C. Günther and M.A. Danzer, *Applied Energy*, 155 (2015) 455
17. H. Liu, Z. Li, Y. Liang, R. Fu and D. Wu, *Carbon*, 84 (2015) 419
18. S.-M. Oh, S.-T. Myung, J. Hassoun, B. Scrosati and Y.-K. Sun, *Electrochemistry Communications*, 22 (2012) 149
19. B. Ellis, W. Makahnouk, Y. Makimura, K. Toghill and L. Nazar, *Nature materials*, 6 (2007) 749
20. T.J. Richardson, *Journal of power sources*, 119 (2003) 262
21. K. Trad, D. Carlier, L. Croguennec, A. Wattiaux, M. Ben Amara and C. Delmas, *Chemistry of Materials*, 22 (2010) 5554
22. L. Fu, Y. Zheng and A. Wang, *Int. J. Electrochem. Sci*, 10 (2015) 3518
23. Y. Lu, L. Wang, J. Cheng and J.B. Goodenough, *Chemical communications*, 48 (2012) 6544
24. Y. Zheng, L. Fu, A. Wang and W. Cai, *Int. J. Electrochem. Sci*, 10 (2015) 3530
25. L.S. Plashnitsa, E. Kobayashi, Y. Noguchi, S. Okada and J.-i. Yamaki, *Journal of The Electrochemical Society*, 157 (2010) A536
26. P. Senguttuvan, G. Rousse, H. Vezin, J.-M. Tarascon and M. Palacín, *Chemistry of Materials*, 25 (2013) 2391
27. Q. Liu, D. Wang, X. Yang, N. Chen, C. Wang, X. Bie, Y. Wei, G. Chen and F. Du, *Journal of Materials Chemistry A*, 3 (2015) 21478
28. W. Song, X. Ji, J. Chen, Z. Wu, Y. Zhu, K. Ye, H. Hou, M. Jing and C.E. Banks, *Phys Chem Chem Phys*, 17 (2015) 159
29. B. Zhang, R. Dugas, G. Rousse, P. Rozier, A.M. Abakumov and J.-M. Tarascon, *Nature communications*, 7 (2016)
30. N. Eshraghi, S. Caes, R. Cloots and F. Boschini, *Scientific congresses and symposiums*, University of Mons (2015)
31. N.P. Aguilar, L.C.T. González, E.M.S. Cervantes, R.K. Gover and L.L. Garza-Tovar, Pechini Synthesis of Na3V2 (PO4) 2F3/C Doped with Aluminum As Cathode for Lithium Ion Batteries, Meeting Abstracts, The Electrochemical Society, 2015, pp. 297.
32. J. Barker, R. Gover, P. Burns and A. Bryan, *Electrochemical and Solid-State Letters*, 9 (2006) A190

33. R. Gover, A. Bryan, P. Burns and J. Barker, *Solid State Ionics*, 177 (2006) 1495
34. W. Massa, O.V. Yakubovich and O.V. Dimitrova, *Solid State Sci.*, 4 (2002) 495
35. A. Tsirlin, R. Nath, A. Abakumov, Y. Furukawa, D. Johnston, M. Hemmida, H.-A.K. von Nidda, A. Loidl, C. Geibel and H. Rosner, *Physical Review B*, 84 (2011) 014429
36. W. Song, X. Ji, C. Pan, Y. Zhu, Q. Chen and C.E. Banks, *Phys Chem Chem Phys*, 15 (2013) 14357
37. W. Song and S. Liu, *Solid State Sci.*, 15 (2013) 1
38. R. Shakoor, D.-H. Seo, H. Kim, Y.-U. Park, J. Kim, S.-W. Kim, H. Gwon, S. Lee and K. Kang, *Journal of Materials Chemistry*, 22 (2012) 20535
39. M. Bianchini, F. Fauth, N. Brisset, F. Weill, E. Suard, C. Masquelier and L. Croguennec, *Chemistry of Materials*, 27 (2015) 3009
40. M. Bianchini, N. Brisset, F. Fauth, F. Weill, E. Elkaim, E. Suard, C. Masquelier and L. Croguennec, *Chemistry of Materials*, 26 (2014) 4238
41. M. Dresselhaus and I. Thomas, *Nature*, 414 (2001) 332
42. J. Choi and A. Manthiram, *Journal of The Electrochemical Society*, 152 (2005) A1714
43. F. Sauvage, E. Quarez, J.-M. Tarascon and E. Baudrin, *Solid State Sci.*, 8 (2006) 1215
44. H. Zhuo, X. Wang, A. Tang, Z. Liu, S. Gamboa and P. Sebastian, *Journal of power sources*, 160 (2006) 698
45. A. Kraytsberg, H. Drezner, M. Auinat, A. Shapira, N. Solomatin, P. Axmann, M. Wohlfahrt-Mehrens and Y. Ein-Eli, *ChemNanoMat*, 1 (2015) 577
46. D.H. Jackson, M.R. Laskar, S. Fang, S. Xu, R.G. Ellis, X. Li, M. Dreibelbis, S.E. Babcock, M.K. Mahanthappa and D. Morgan, *Journal of Vacuum Science & Technology A*, 34 (2016) 031503
47. M. Sahoo, K. Sreena, B. Vinayan and S. Ramaprabhu, *Mater. Res. Bull.*, 61 (2015) 383
48. N. Taguchi, H. Sakaebe, K. Tatsumi and T. Akita, *e-Journal of Surface Science and Nanotechnology*, 13 (2015) 284
49. X.-F. Yang, J.-H. Yang, K. Zaghib, M.L. Trudeau and J.Y. Ying, *Nano Energy*, 12 (2015) 305
50. H. Gwon, D.H. Seo, S.W. Kim, J. Kim and K. Kang, *Adv Funct Mater*, 19 (2009) 3285